

Experimental Observations of Macrosegregation in DC Casting of Rolling Slab Ingots

S.R. Wagstaff and A. Allamore

Department of Materials Science and Engineering

Massachusetts Institute of Technology, 77 Massachusetts Ave. Cambridge, MA 02139

The increased demand for aluminum as a primary structural metal stems from a quest in automotive, aerospace, and marine industries to be more energy efficient and sustainable. This unprecedented demand drives aluminum casting methods towards increased productivity looking to, cast larger ingots faster. The unfortunate consequence of this approach is an enhanced variation of metallurgical properties over the cross section of slab ingots. Rolling slab ingots of AlCu4.5 using a typical Direct-Chill casting technique have been cast and sectioned for analysis. This alloy allowed us to compare our results with the available literature and to elucidate the marked differences in spatial variation of microstructure and composition found in radial and lateral symmetry castings. In an attempt to couple conventional theory with our results, sump and temperature profiles were measured in-situ and modeled using a commercial finite element analysis software package. The combination of experimental and modeling results indicate that the variations in the cooling parameters through the cross section are largely responsible for the spatial variances in metallurgical properties, pointing to a possible refinement of DC casting parameters.

Direct-chill (DC) casting of aluminum is one of the most important process developments that has taken place in the aluminum industry in the past 100 years. It has increased the productivity, reliability, and consistency of certain products far beyond the capabilities of previous technology. Yet, in spite of all of the advances made in casting technology there are still considerable obstacles to overcome before some products can be reliably produced.

Macroscopic segregation is a common metallurgical defect in DC casting of aluminum alloys. It is characterized by variations in composition on a length scale larger than the as solidified grains within the casting. This variation in composition is magnified in large castings, and can subsequently affect the material properties. Unlike microsegregation, which comprises compositional variances at the grain scale, downstream processing cannot mitigate macrosegregation's effects. As a result, if not properly understood and controlled, macrosegregation can lead to downstream rejection of the cast.

Macroscopic segregation, can generally be understood as the relative movement of solid and liquid phases of different composition. The inhomogeneous movement of these phases leads to the gradual change in composition throughout the ingot. Considerable research has been conducted on the specific mechanisms behind macrosegregation, and it is generally considered to be the result of the following processes, possibly acting in concert:

1. The precipitation of solid (or liquid) phases and their respective displacement. (*Sedimenting grains*)

2. Flow of the liquid phase within the semi-solid (mushy) zone due to volume change upon freezing (*Shrinkage induced flow*).

3. Natural convection resulting from thermal, or solutal stratification during the casting process.

4. Deformation of the solid network due to mechanically or thermally induced stresses.

The first process occurs due to the non-equilibrium solidification conditions present in DC casting. This refers to the nucleation of primary phase crystals which are poor in solute and are then preferentially deposited throughout the casting. Macroscopic segregation in this case, only occurs after the crystals have settled out of solution and adhered to the solidifying interface [1].

The second process is due to the volume change associated with solidification of metals. The density increase upon phase change causes liquid to flow between the dendrites, perpendicular to the temperature isotherms towards the interface. Since the liquid adjacent to the interdendritic channel is enriched in solute, the result is an enrichment of the two phase region, and can result in positive surface and negative centerline segregation [2,3,4].

The third mechanism arises because of the density of the dendrites and interdendritic liquid differ. This gives rise to convective currents, and thus macrosegregation. The compositional variance occurs because solute is transported from one part of the two phase region to another, or due to channel formation allowing solute to enrich the bulk liquid [1,5,6,7].

The fourth mechanism occurs when a stress is placed upon the dendrite network. The resulting strain causes solute to enter or leave the two phase region similar to what occurs in shrinkage induced flow. Typically in DC casting, stresses occur in the matrix due to mechanical deformation caused by non-uniform cooling (ex: *butt curl*)[8].

Analytic models of macrosegregation, assuming other mechanisms do not operate, have been proposed for some of the aforementioned mechanisms. The Burton, Prim and Slichter methodology [9] can be used to describe rejection of solute into an homogenous, perfectly mixed, bulk liquid. Kirkaldy and Youdelis [10], as well as Flemings and Nereo [11] proposed a model based on the volume change during solidification (*normal freezing*). Mehrabian et al [12] attempted to model more complex convective conditions, but their analysis did not include the effects of solute return.

The complex interplay between the various mechanisms of macrosegregation make accurate modeling a formidable challenge. With advances in computer technology, finite element models have been used and developed by various researchers to couple all of the mechanisms into a single model. For example, Krane et al [13] have developed a model capable of accounting for fluid flow due to convection and shrinkage as well as primary phase precipitation. These models are remarkable in their ability to predict and match macrosegregation patterns. Unfortunately as often in casting literature, the computed results are lacking experimental validation. One of the principle reasons for this is the general lack of controlled, experimental data especially relating to rolling slab ingots. Typically, results are presented for smaller diameter billets because one can rely on the radial symmetry of the system to aid analysis efforts. The radial symmetry present in billets adds to the inherent complexity of the problem, and because variations in the number of precipitated grains in the conical billet sump were difficult to track and did not affect the width of the solute poor region significantly. This idea can be seen conceptually in Figure 1. As the number density of precipitated grains increases within the sump for any number of reasons, the width of the depleted region increases at a lower rate, thereby making experimental observations of precipitating grains and their effect on macrosegregation, extremely difficult. Additionally, precipitated grain density is extremely difficult to control experimentally and thus had to be observed post-mortem. Chu and Jacoby studied rolling slab ingots and reinvigorated the sedimenting grain theory, but their data was limited to a single trace from the rolling face to the center of the ingot [14]. Among the problems with macrosegregation measurements are the great cost of production and difficulties in sectioning and sampling large

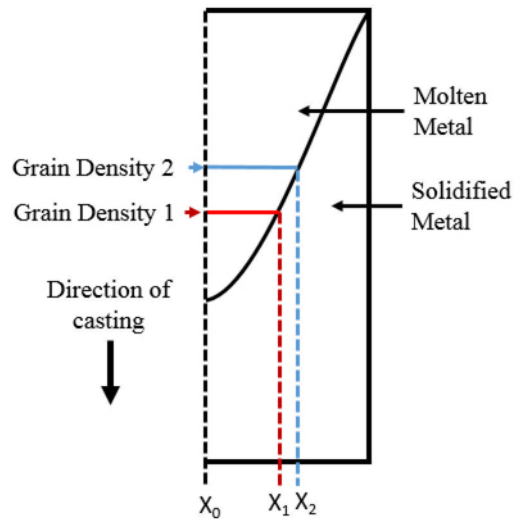


Figure 1: Schematic representation of the small change in central depleted zone width with increased precipitated grain density.

ingots. Finally, there is a lack of experimental casting data for binary alloys to compare with computed results, since commercial alloys tend to be more complex. As a first step to fulfill the lack of experimental data, this paper presents results obtained during the sectioning of an industrial size AlCu4.5 ingot.

Experimental Procedure

For this experiment, a charge of Al4.5Cu was loaded into a commercial gas burner furnace. The melt was degassed, filtered and grain refined (25 ppm) following available commercial standards. The metal was then cast using a bi-level pour method through a downspout and combination bag into a 1750x600mm WAGSTAFF LHC™ open top mold. The casting speed was 65 mm/min, (the reader is directed to additional papers regarding the physical properties of this alloy) and a series of thermocouple rakes were inserted into the melt in order to capture the cooling and solidification conditions present during the steady state casting.

The cold ingot was then sectioned both longitudinally and in cross section. The cross section was divided into quadrants and a series of 45 samples were removed using a core drill for analysis (see Figure 2). Samples were also taken from the longitudinal slice approximately every 6 inches from the bottom (*butt*) to the top (*head*) of the ingot. After sectioning, the samples were analyzed for composition using optical emission spectroscopy, and then processed using an SEM to analyze grain size and

secondary dendrite arm spacing using the line intercept method [15].

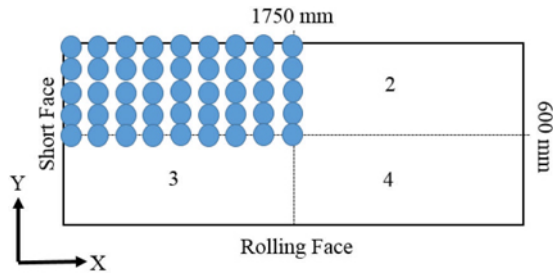


Figure 2: Locations of samples taken from cross section of ingot in quadrant 1. Bilateral symmetry allows sampling from one quadrant.

Results and Discussion

Typically, macrosegregation profiles in a radially symmetric billet mold exhibit a “W” shaped profile for Al4.5%Cu and similar alloys. The strong negative segregation present in the center of the castings distinguishes this alloy series from others, and prompted some of the initial interest in macrosegregation in DC casting. The cause of this segregation has been the subject of much debate, but to date the consensus is that this centerline segregation is dominantly caused by the precipitation of primary phase particles. Figure 3 is a representation of the macrosegregation contour for one quarter of the ingot cross section. The composition from each position is normalized to the furnace composition, and is presented as a percent deviation. Consistent with previous results for this alloy is the large, nearly linear, depleted region located in the center of the ingot parallel to the rolling face. In order to better understand this result, an additional cast was made under identical conditions, but molten zinc was poured into the sump in steady state to preserve the shape of the solidification front. After slicing and etching, the solidification front was plotted. The resulting cross sections are presented in figures 4a and b. Figure 4a is presented in the XZ plane, facing the rolling face. Figures 3 and 4a allow us to determine the location of the depleted zone in the x-direction of the sump cross section. The start of the depleted zone is labeled X_1 in both figures. A similar procedure has been conducted in the y-direction for Figures 3 and 4b (mark Y_1). Examination of these points indicates that the depleted zone falls uniquely in the lowest portion of the sump, where sedimenting grains are most likely to precipitate, thereby forming the depleted central zone.

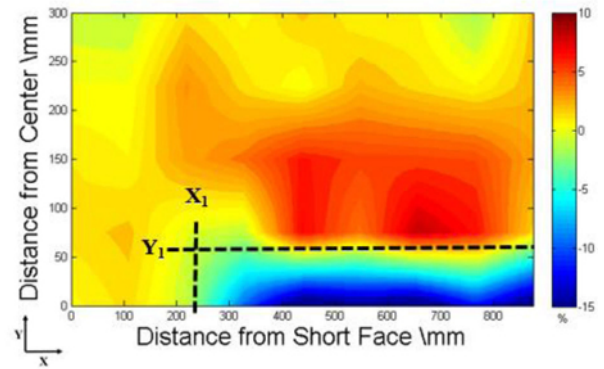


Figure 3: Macrosegregation contour for quadrant 1

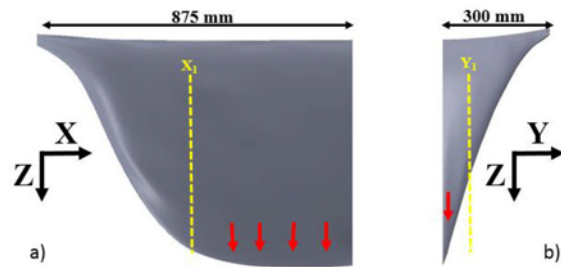


Figure 4: 2D representations of zinc sump facing: a) towards the rolling face, b) towards the short face. Arrows indicate sedimentation zones. Line positions X_1 and Y_1 correspond to those of figure 3.

Figure 5 is a representation of the longitudinal macrosegregation through the length of the ingot. The degree of negative centerline segregation varies with position during the cast, with local maxima at both the beginning and end of the cast. While a change in

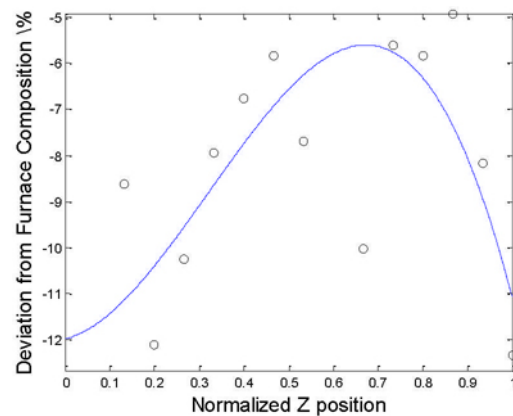


Figure 5: Centerline macrosegregation along normalized ingot length. Blue line is a trendline to aid examination.

macrosegregation is expected during the course of the cast, it is generally assumed that the macrosegregation pattern follows the casting procedure and increases with increasing sump depth. Our data suggests that macrosegregation is actually magnified at the beginning and end of the cast, where the sump depth is shallowest and horizontal shrinkage flow should be the least. A possible explanation for this is also related to precipitated primary grains. At the beginning of a cast, numerous primary phase grains are nucleated as molten metal flows into the mold. Shallow sump depths lead to increased nucleation as the molten metal, directed by the combo bag, flows over the freshly solidified metal and dendrite arms are fragmented and drawn into the melt. A slurry of primary phase particles may result from such effects, which continue to grow in the melt pool until a critical grain size is achieved and they are precipitated out. At the end of the cast, no new metal is added and the bulk liquid continues to cool without forced stratification. This leads to increased grain nucleation and preferential precipitation.

Figures 6 and 7 are representations of dendrite arm spacing and grain size for the quarter slice of the cross section. These plots are qualitatively similar, both parameters being influenced nearly linearly by cooling rate.

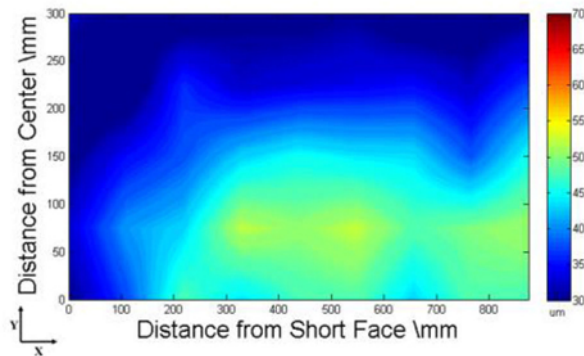


Figure 6: Secondary dendrite arm spacing for quadrant 1 (μm).

These two figures illustrate the existence of regions of larger particle size between the center and the rolling face. This is consistent with the sump measurement, since this position corresponds to the inflection point of the profile, and thereby corresponds to the longest solidification time. Knowing that particles are largest in this area, we can explain the zone of positive macrosegregation in a similar position in Figure 3.

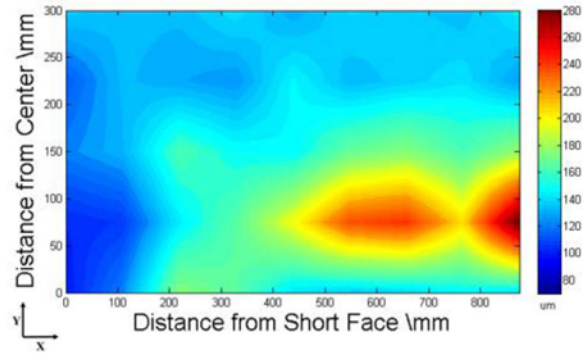


Figure 7: Grain size for quadrant 1 (μm).

Numerous relations exist to model the shrinkage induced flow present in the mushy zone of solidifying castings, but it is accepted that larger particle size leads to a larger permeability. This increased permeability then correlates to an increase in shrinkage induced flow. Since the region adjacent to the front is richer in rejected solute, it is this material drawn into the mushy zone that leads to the increased copper concentration in the region between the center and the rolling face.

The absence of a solute rich zone is noticeable in Figure 3 between the short face and the center. Figure 8 is a finite element model generated using ANSYS Fluent software, for the same quarter section. The fluid dynamic calculations were done using a standard $k-\epsilon$ turbulence model. Material properties were taken from tabulated properties available in the literature¹⁶. The mushy zone region properties were interpolated by the software based on local temperature and the corresponding fraction solid as defined by the Scheil equation. Thermal boundary conditions within the mold were calculated from thermal data in the inverse method described by Drezet et al [17]. Figure 9 is a plot of the corresponding heat flux for the rolling face. It was found that the boundary condition varied from the short face to the rolling face, the measured ratio (short face/rolling face) being ~ 1.35 . This change in cooling rate may be partially responsible for the decreased permeability (larger particle size) between the center and the short face. The increased cooling decreases the magnitude of the slope of the interface thereby increasing the effective cooling rate and decreasing grain size.

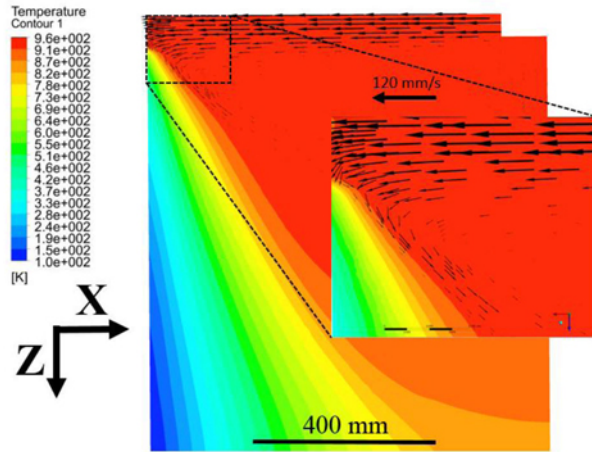


Figure 8: A temperature contour plot illustrating the thermal profile within the sump. Velocity vectors are sized according to magnitude.

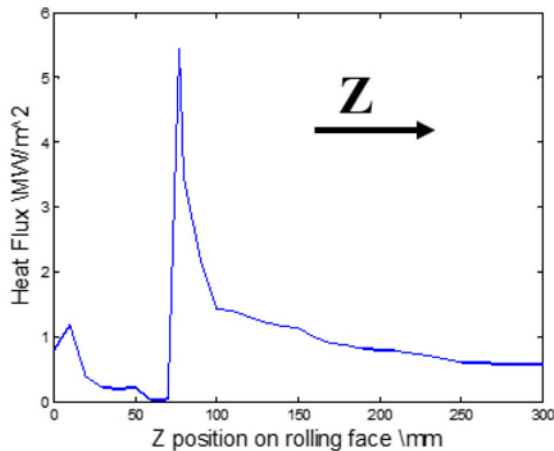


Figure 9: Measured heat flux profile for ingot along rolling face.

Observable in Figure 8 is a temperature contour illustrating the thermal profile within the sump. The liquidus temperature for this alloy is 933K and the solidus is 822K. Velocity vectors are superimposed on the thermal profile to indicate flow direction and magnitude. As a consequence of the chosen distribution bag, the bulk of the molten metal is directed to the short face along the surface. As a consequence, metal impacts the short face and a certain portion recirculates in the XY plane and flows parallel to the rolling face. However, the remainder of the metal redirects downward along the solidification front adjacent to the short face. The consequence of this flow may be the redistribution of the primary phase particles from the slurry zone (incoherent zone) towards the center, thereby contributing to the negative centerline segregation. In addition, as the metal progresses parallel to the

solidification front, rejected solute is redistributed adjacent to, and within the mushy zone. In the absence of a bulk quantity of solute rich material to feed the interdendritic channels, more homogeneous material is drawn to the solidification front, thereby inhibiting the formation of a solute rich region between the short face and the center.

Conclusions

Macrosegregation in the DC casting of rolling slab ingots has been investigated, using a combination of experimental and computational methods. A macrosegregation profile through the cross section of an industrial rolling slab ingot, shows that macrosegregation in such castings cannot be properly illustrated through a line plot. The complex interplay between fluid flow and precipitation becomes magnified in such large scale. In a first modeling attempt of our results, we showed that it is possible for the fluid dynamic conditions of the mold to affect grain and solute distributions within a casting. We have also shown that the non-uniform heat transfer conditions from the short face to the rolling face can contribute to a layered structure within rolling slab ingots. This information indicates that cooling conditions within the mold could continue to modify macrosegregation profiles. More work is underway to understand the effects of fluid flow within the mushy zone, its effects on grain and solute transport, and how such phenomena can affect macrosegregation.

A special thanks to the NOVELIS Solatens team for the use of their facility as well their support and assistance throughout the course of this study.

¹ Yu H, Granger DA. In: Starke Jr EA, Sanders Jr TH, editors. *International conference on aluminum alloys – their physical and mechanical, properties*. Warley, UK: EMAS; 1986. pp. 17–29.

² A.V. Reddy, C. Beckermann. In: Voller VR, El-Kaddah N, Marsh SP, editors. *Materials processing in the computer age II*. Warrendale [PA]: TMS; 1995. p. 89–102.

³ Drezet J-M, Gremaud M, Rappaz M. In: Muller HR, editor. *Continuous casting*. Weinheim: Wiley-VCH; 2005. p. 151–61.

⁴ Du Q, Eskin D, Katgerman L. In: Gandin Ch.A, Bellet M, editors. *Modeling of casting, welding and advanced solidification processes XI*, TMS, Warrendale [PA], 2006. p. 235–242.

⁵ Beckermann C. *Int Mater Rev*, 2002, vol. 47: pp 243–61.

⁶ Du Q, Eskin DG, Katgerman L. *Metall Mater Trans A* 2007;vol 38. pp 180–9.

⁷ Flood SC, Katgerman L, Voller VR: In Rappaz M, Ozgu MR, Mahin KW, editors. *Modeling of casting, welding and advanced solidification processes V*. Warrendale: TMS, PA; 1991, pp. 683–90.

-
- ⁸ Nicolli LC, Mo A, M'Hamdi M. *Metall Mater Trans A* 2005; vol 36A: pp. 433–42.
- ⁹ J.A. Burton, R.C. Prim, and W.P. Slichter: *J. Chem. Phys.*, 1953, vol. 21, p. 1987.
- ¹⁰ J.S. Kirkaldy and W.V. Youdelis: *Trans. TMS-AIME*, 1958, vol. 212, p. 833.
- ¹¹ M.C. Flemings and G.E. Nereo: *Trans. TMS-AIME*, 1967, vol. 239, p. 1449.
- ¹² R. Mehrabian, M. Keane, and M.C. Flemings: *Met Trans.*, 1970, vol. 1, p. 1209.
- ¹³ M. J. M. Krane, *Appl. Math. Modelling*, 2004, vol. 28, pp. 95-107.
- ¹⁴ Chu MG, Jacoby JE. In: Bickert CM, editor. *Light metals*. Warrendale [PA]: TMS; 1990. p. 925–30.
- ¹⁵ ASTM Standard E112 – 13 available at: <http://www.astm.org/Standards/E112.htm>
- ¹⁶ Krane M J M and Vušanović I *Mater. Sci. Tech.* 2009. vol. 25. pp. 102.
- ¹⁷ Drezet, J. M., Rappaz, M. M., Grun, G. U., & Gremaud, M. M. *Metallurgical And Materials Transactions A (Physical Metallurgy And Materials Science)*, (2000). Vol. 31A(6), 1627-1634.